

Prepared for Headquarters, U.S. Army Corps of Engineers

The contents of this report are not to be used for advertising, publication, or promotional purposes. Citation of trade names does not constitute an official endorsement or approval of the use of such commercial products.

The findings of this report are not to be construed as an official Department of the Army position, unless so designated by other authorized documents.



PRINTED ON RECYCLED PAPER

Quantitative Analysis of the Detection Limits for Heavy Metal-Contaminated Soils by Laser-Induced Breakdown Spectroscopy

by Dennis R. Alexander, Dana E. Poulain

University of Nebraska-Lincoln
248 WSEC, Box 880511
Lincoln, NE 68588-0511

Final report

Approved for public release; distribution is unlimited

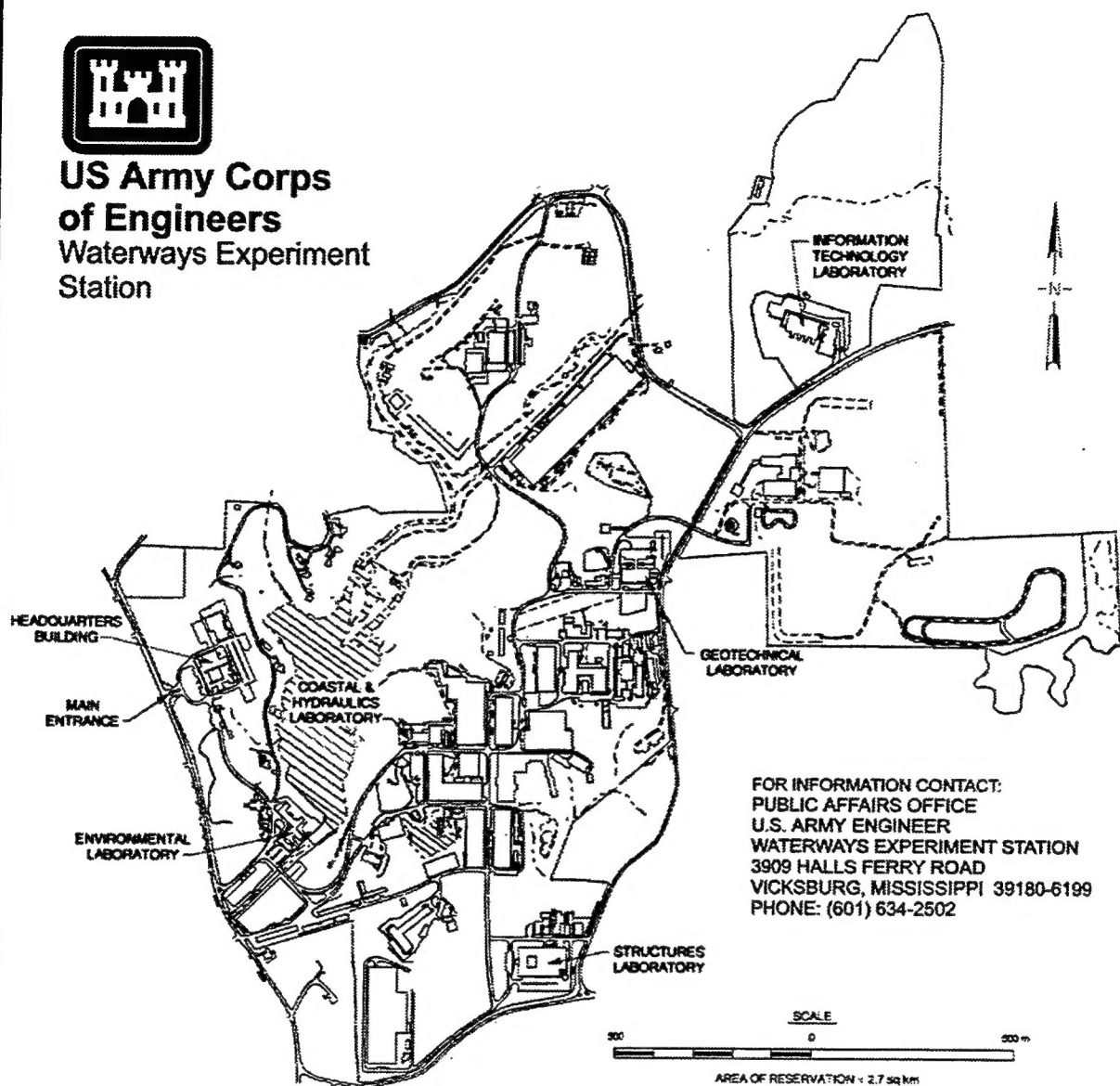
DTIC QUALITY INSPECTED 3

Prepared for **U.S. Army Corps of Engineers
Washington, DC 20314-1000**

Monitored by **U.S. Army Engineer Waterways Experiment Station
3909 Halls Ferry Road, Vicksburg, MS 39180-6199**



**US Army Corps
of Engineers**
Waterways Experiment
Station



Waterways Experiment Station Cataloging-in-Publication Data

Alexander, Dennis R.

Quantitative analysis of the detection limits for heavy metal-contaminated soils by laser-induced breakdown spectroscopy / by Dennis R. Alexander, Dana E. Poulain ; prepared for U.S. Army Corps of Engineers ; monitored by U.S. Army Engineer Waterways Experiment Station.

33 p. : ill. ; 28 cm. -- (Miscellaneous paper ; IRRP-97-2)

Includes bibliographic references.

1. Laser spectroscopy. 2. Soil pollution -- Measurement. 3. Soils -- Environmental aspects. I. Poulain, Dana Earl. II. United States. Army. Corps of Engineers. III. U.S. Army Engineer Waterways Experiment Station. IV. Installation Restoration Research Program. V. Series: Miscellaneous paper (U.S. Army Engineer Waterways Experiment Station) ; IRRP-97-2.

TA7 W34m no.IRRP-97-2

Contents

Preface	vi
Summary	vii
1—Introduction	1
2—Experimental Method	2
Sample Preparation	2
LIBS System	5
3—Results	6
Soil Compression Effects	6
Excitation Source	7
Calibration Data	20
Detection Limits	20
4—Conclusions	22
References	23
SF 298	

List of Figures

Figure 1. Comparison of dried sand samples with 50 ppm of Cr, as ammonium dichromate, and doped with an equivalent volume of distilled water	3
Figure 2. Photograph showing detail of sand cross section from Figure 1, doped with 50 ppm Cr	3
Figure 3. Photographs showing surface details of sand samples doped with 50 ppm Cr compared with reference sand with 0 ppm Cr	4
Figure 4. Schematic of a typical LIBS system using a Nd:YAG laser and an optical multichannel analyzer	5
Figure 5. Effect of "relaxation time" after soil compression on LIBS measurements of 50 ppm Cr in sand	6

Figure 6.	Comparison of calibration curves for Pb in clay, based on intensity ratio of Pb-I to Si-I, obtained for Nd:YAG and excimer laser sources	7
Figure 7.	Emission spectrum showing relevant atomic emission lines of As and Si used in LIBS calibration . .	8
Figure 8.	Plot of signal-noise ratio of As-I line to background in vicinity of 245 nm as a function of ICCD gate delay time	8
Figure 9.	Calibration curves for As in (a) sand, (b) silt, (c) clay, and (d) kaolin, based on intensity ratio of As-I to Si-I	9
Figure 10.	Emission spectrum showing relevant atomic emission lines of Cd and Ti used in LIBS calibration . .	10
Figure 11.	Plot of signal-noise ratio of Cd-I line to background in vicinity of 510 nm as a function of ICCD gate delay time	10
Figure 12.	Calibration curves for Cd in (a) sand, (b) silt, (c) clay, and (d) kaolin, based on intensity ratio of Cd-I to Ti-I	11
Figure 13.	Emission spectrum showing relevant atomic emission lines of Cr and Si used in LIBS calibration . .	12
Figure 14.	Plot of signal-noise ratio of Cr-I line to background in vicinity of 417 nm as a function of ICCD gate delay time	12
Figure 15.	Calibration curves for Cr in (a) sand, (b) silt, (c) clay, and (d) kaolin, based on intensity ratio of Cr-I to Si-I	13
Figure 16.	Emission spectrum showing relevant atomic emission lines of Hg and Ti used in LIBS calibration . .	14
Figure 17.	Plot of signal-noise ratio of Hg-I line to background in vicinity of 460 nm as a function of ICCD gate delay time	14
Figure 18.	Calibration curves for Hg in (a) sand, (b) silt, (c) clay, and (d) kaolin, based on intensity ratio of Hg-I to Ti-I	15
Figure 19.	Emission spectrum showing relevant atomic emission lines of Pb and Si used in LIBS calibration . .	16

Figure 20. Plot of signal-noise ratio of Pb-I line to background in vicinity of 409 nm as a function of ICCD gate delay time	16
Figure 21. Calibration curves for Pb in (a) sand, (b) silt, (c) clay, and (d) kaolin, based on intensity ratio of Pb-I to Si-I	17
Figure 22. Emission spectrum showing relevant atomic emission lines of Zn and Ti used in LIBS calibration . .	18
Figure 23. Plot of signal-noise ratio of Zn-I line to background in vicinity of 479 nm as a function of ICCD gate delay time	18
Figure 24. Calibration curves for Zn in (a) sand, (b) silt, (c) clay, and (d) kaolin, based on intensity ratio of Zn-I to Ti-I	19

Preface

The work reported herein was conducted by the University of Nebraska at Lincoln for the U.S. Army Engineer Waterways Experiment Station (WES). The research was sponsored by the Headquarters, U.S. Army Corps of Engineers (HQUSACE) Installation Restoration Research Program (IRRP), Environmental Quality and Technology Applied Research Work Unit entitled "Advanced Sensor Systems for the Cone Penetrometer System," Project AF25-CT-004. Dr. Clem Meyer was the IRRP Coordinator at the Directorate of Research and Development, HQUSACE. Dr. M. John Cullinane, Jr., WES, was the IRRP Program Manager.

The laboratory studies were conducted and the report herein prepared by Dr. Dana E. Poulain under the guidance of Dr. Dennis R. Alexander, both of the University of Nebraska.

At the time of publication of this report, Director of WES was Dr. Robert W. Whalin. Commander was COL Bruce K. Howard, EN.

This report should be cited as follows:

Alexander, D. R., and Poulain, D. E. (1997). "Quantitative analysis of the detection limits for heavy metal-contaminated soils by laser-induced breakdown spectroscopy," Miscellaneous Paper IRRP-97-2, U.S. Army Engineer Waterways Experiment Station, Vicksburg, MS.

The contents of this report are not to be used for advertising, publication, or promotional purposes. Citation of trade names does not constitute an official endorsement or approval of the use of such commercial products.

Summary

Laser-induced breakdown spectroscopy (LIBS) is a rapid remote measurement method for detection of metals in the environment. A major factor in the quantitative use of this technique involves the minimum detection limits under both laboratory and field operations. Research on limits of detection of heavy metals in different types of soils under various conditions using LIBS has been carried out under Contract DACA39-95-K-0053. Pulses from a Nd:YAG laser operating at 125 mJ at $\lambda = 1.06 \mu\text{m}$ are focused on sample surfaces to produce laser sparks (plasmas). Atomic emissions from the plasmas are recorded using an optical multichannel analyzer after delays of a few microseconds when interference from broad-band emissions is reduced.

Research has been performed on the detection limits of arsenic, cadmium, chromium, mercury, lead, and zinc in soil matrices. Results are reported on the lower detection limits of these six elements in sand, silt, clay, and kaolin matrices. Detection limits are significantly lower for heavy metals in sand matrices than silt and clay matrices due to differences between surface and volume contamination.

An excimer laser operating at 125 mJ at $\lambda = 248 \text{ nm}$ was used to provide a comparative LIBS analysis for Pb in a silt matrix. No significant difference in the lower detection limit was obtained by using an excimer laser as the excitation source in place of the Nd:YAG laser.

The LIBS method must provide accurate data when used in a cone penetrometer. Conditions that would be encountered by a cone penetrometer-based LIBS system have been simulated by compressing soil samples and then allowing them to relax for specific intervals before LIBS analysis. Results are presented of the dependence of LIBS measurements on the relaxation time after soil sample compression. These data are important in order to have a firm understanding of lower detection limits for field-deployable LIBS systems.

1 Introduction

Recently, interest in sensors to accurately assess and monitor the extent of environmental contamination around waste disposal sites and research facilities has grown markedly. There is an ever-increasing need to quickly and accurately perform concentration measurements of chemical species in situ. Previously, these measurements could only be performed in the laboratory. However, the volume of measurements to be performed today and in the future has a prohibitive cost of time and finances to acquire soil or water samples and return them to a laboratory for analysis. Thus, new methods are needed to perform remote measurements quickly and efficiently, while maintaining comparable analysis capabilities.

Laser-induced breakdown spectroscopy (LIBS) is one method with the potential to satisfy these requirements. In this method the laser source serves to vaporize, atomize, and excite the sample material in the course of one laser pulse. This method has been used in analyses of gases (Cremers and Radziemski 1983), liquids (Cremers, Radziemski, and Loree 1984; Wachter and Cremers 1987), solids (Grant, Paul, and O'Neill 1991), solid aerosols (Radziemski et al. 1983; Ottesen et al. 1991; Flower et al. 1994), liquid aerosols (Archontaki and Crouch 1988; Holtzclaw, Moore, and Senior 1993; Poulain and Alexander 1995), and soils (Wisbrun et al. 1994; Alexander et al. 1993; Cremers, Barefield, and Koskelo 1995; Alexander et al. 1996). Because of the relative simplicity of LIBS, it is well suited for use in the field. One existing field-deployable site characterization system to which LIBS could be adapted is the Site Characterization and Cone Penetrometer System (SCAPS) developed by the U.S. Army Engineer Waterways Experiment Station (WES). SCAPS sensors, housed in a cone penetrometer, are driven into the soil by a hydraulic ram to depths of up to 60.96 m (200 ft). Measurements are performed in situ during the descent and/or ascent of the penetrometer. Thus, there is the potential to determine contaminant plume boundaries onsite.

As part of an ongoing effort to develop LIBS for use with SCAPS, the current work reports lower detection limits for arsenic (As), cadmium (Cd), chromium (Cr), mercury (Hg), lead (Pb), and zinc (Zn) in sand, silt, clay, and kaolin matrices. Also, several influences on LIBS concentration measurements of these heavy metals in the various matrices are discussed.

2 Experimental Method

Sample Preparation

Four soil or soillike matrices were considered in this investigation: sand, silt, clay, and kaolin. The materials and corresponding suppliers are noted in Table 1. Washed and dried sand (Mallinckrodt Chemical, Inc.,

Table 1
Summary of Soil Matrices Used
in Detection Limit Analysis

Type	Supplier Soil
Sand	Mallinckrodt Chemical, Inc., No. 7062
Silt	WES
Clay	WES
Kaolin	Mallinckrodt Chemical, Inc., No. 5645

No. 7062 KPTN) was used in place of "Yuma" sand (obtained from WES) because the sand was found to already contain up to 4 ppm chromium. Silt, obtained from WES, was used as supplied. Clay, also obtained from WES, was sifted through a 1-mm mesh to remove large granular materials prior to doping with heavy metals. Kaolin (Mallinckrodt Chemical, Inc., No. 5645) is the principal component of kaolinite clay. It is a hydrous silicate of aluminum. Kaolin was used in this work because it approximates a relatively "pure" clay. Contamination of the soil matrices was accomplished by doping the samples with solutions of the heavy metals at various concentrations to achieve the desired parts per million (by mass) of the metals to the soils. The compounds used to produce the solutions of the six heavy metals are noted in Table 2.

Table 2
Summary of Solutions Used
for Doping Soil Matrices Used
in Detection Limit Analysis

Element	Source Chemical
As	arsenic trioxide (As_2O_3)
Cd	cadmium chloride ($\text{CdCl}_2 \cdot 2.5\text{H}_2\text{O}$)
Cr	ammonium dichromate ($(\text{NH}_4)_2\text{Cr}_2\text{O}_7$)
Hg	mercuric chloride (HgCl_2)
Pb	lead nitrate ($\text{Pb}(\text{NO}_3)_2$)
Zn	zinc chloride (ZnCl_2)

The compounds were each dissolved in distilled water to produce a primary solution. For each soil sample, solutions were prepared such that addition of 10 ml of the solution to 50 g of soil would result in a concentration of heavy metal in the soil between 100 parts per billion (ppb) and 2,000 parts per million (ppm). Diluted solutions were derived from the primary solutions by dilution with distilled water.

An important consideration in the sample preparation process became evident during preparation of the chromium

samples. Due to the strong yellow-orange color of the ammonium dichromate solution, inhomogeneities of the sample were plainly visible at higher doping concentrations (approximately 5 ppm and greater). Shown in Figure 1 are petri dishes containing sand samples with 50 ppm Cr (left) and 0 ppm Cr (right).

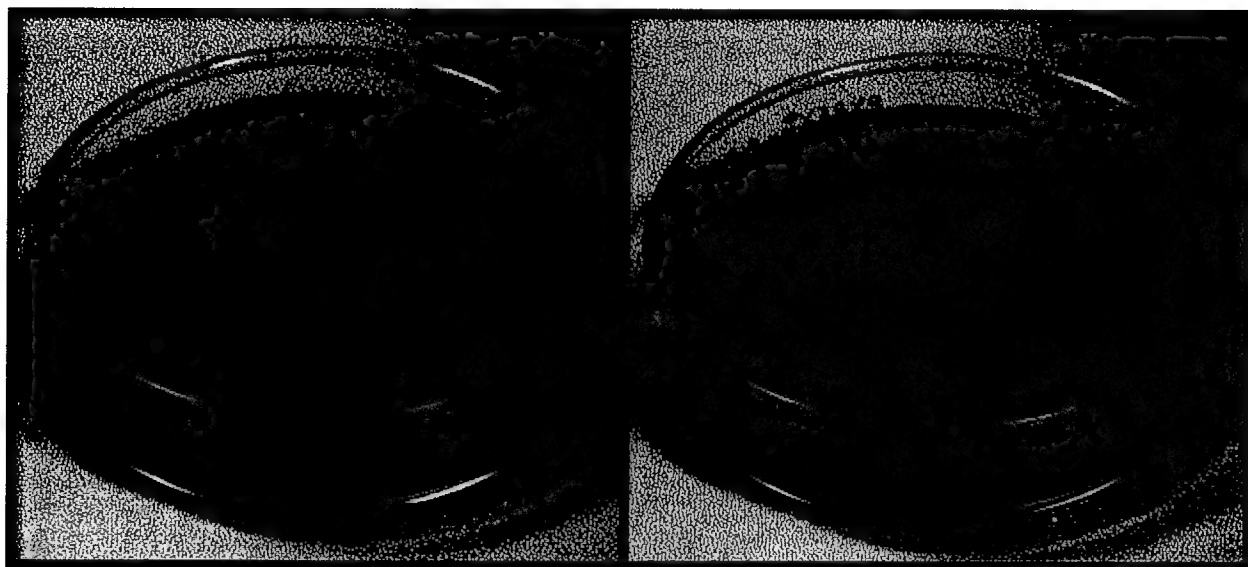


Figure 1. Comparison of dried sand samples (left) with 50 ppm of Cr, as ammonium dichromate, and (right) doped with an equivalent volume of distilled water

The sample with 50 ppm Cr has a noticeably more intense color on the surface of the sample. A detailed view of the sample through the wall of the petri dish is shown in Figure 2. In this figure, it is observed that the chromium appears to be concentrated in the top 1 mm of the sample.

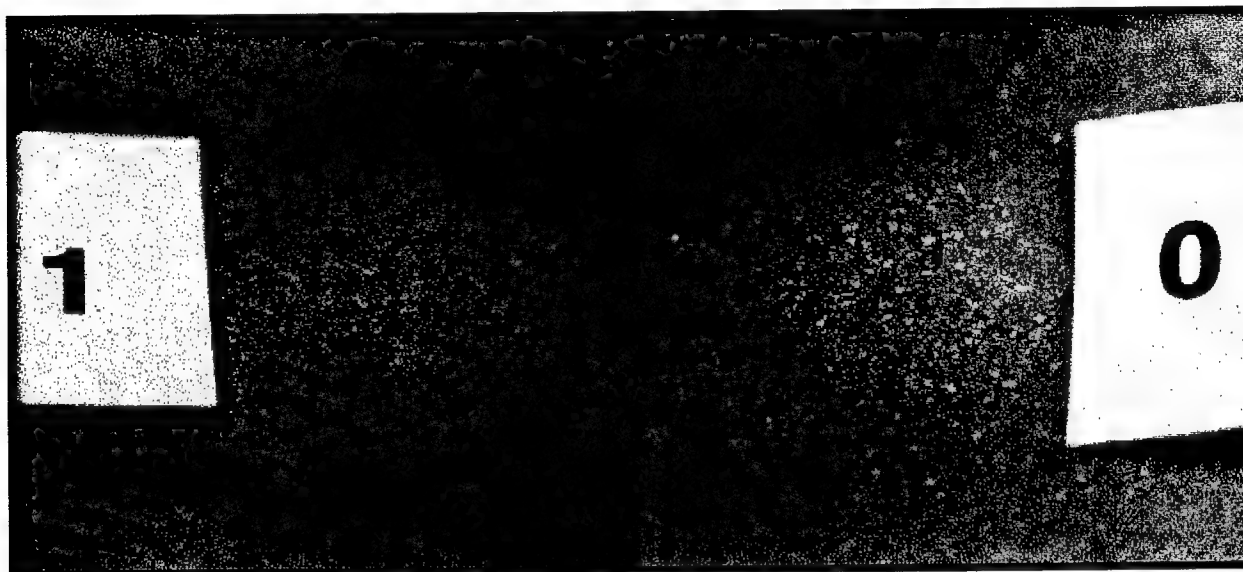


Figure 2. Photograph showing detail of sand cross section from Figure 1, doped with 50 ppm Cr (as ammonium dichromate)

Shown in Figure 3 are the results of various mixing methods on two chromium-doped sand samples (with a nondoped sand sample for comparison). The photograph in Figure 3(a) is a detail of the surface of a sand sample, doped with 50 ppm Cr, mixed once during the drying interval and then mixed just prior to photographing. The photograph in Figure 3(b) is a detail of the surface of a sand sample, also doped with 50 ppm Cr, but mixed every 10 min during the drying interval. Evident in Figure 3(a) are the localized regions of high chromium concentration. In the context of LIBS calibration, detection limits decrease as the standard deviation of the emission intensity ratios decrease. Comparison of Figure 3(a)(left) and Figure 3(b)(left) suggests that mixing

of the sample only after drying does not distribute the dopant material in the most uniform manner throughout the soil.

Samples in the investigation of compression effects were prepared by placing contaminated soils into aluminum sample holders (wall thickness approximately 0.635 cm (0.25 in.)) and loading with 177.92 kN (20 tons) force in a hydraulic press for a period of 1 min.



(a)



(b)

Figure 3. Photographs showing surface details of sand samples doped with 50 ppm Cr (as ammonium dichromate) (left) compared with reference sand with 0 ppm Cr (right) (mixed once during the drying interval (a), and mixed every 10 min during the drying interval (b))

LIBS System

A schematic of the experimental arrangement used in performing the experimental research is shown in Figure 4.

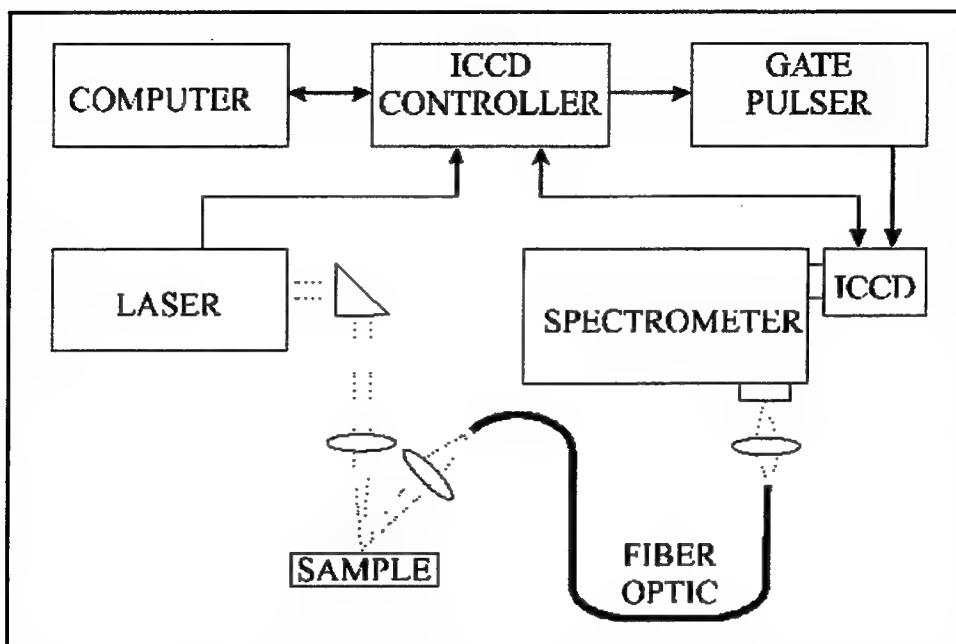


Figure 4. Schematic of a typical LIBS system using a Nd:YAG laser and an optical multichannel analyzer

A pulsed Nd:YAG laser (Big Sky Laser, Model 100R), operating at the principal wavelength ($\lambda = 1.06 \mu\text{m}$) and 10-ns pulse width, serves as the excitation source. The laser radiation is focused by a plano-convex BK7 lens (diameter (ϕ) = 15 mm, focal length (f) = 100 mm) on the soil sample. An optical multichannel analyzer (OMA), consisting of a spectrometer (Instruments SA, Model HR-320, $f = 320 \text{ mm}$) equipped with an intensified CCD camera (ICCD) (Princeton Instruments, Model ICCD-1024MG-E), is used to analyze the spectra of the plasma emissions. Emission from the laser-produced plasma is focused by a fused silica lens into an optical fiber (3M, TECS FT-1.0-UMT) for transmission to the OMA. Transmitted light from the fiber is coupled into the OMA with a bi-convex fused silica lens ($\phi = 25 \text{ mm}$, $f = 50 \text{ mm}$). An aperture between the lens and OMA slit matches the F/# of the lens to the spectrometer. The entrance slit of the spectrometer is typically opened $25 \mu\text{m}$. The region of the plasma imaged by the spectrometer is approximately 1 mm in diameter. The spectrometer is equipped with a 1,200-lines/mm holographically ruled diffraction grating. The OMA was able to acquire individual spectra from the LIB plasma at the rate of approximately two per second. To increase the signal-to-noise ratio for the atomic emission lines, and thus reduce the limits of detection, the ICCD is gated. A Q-switch sync signal from the Nd:YAG triggers a gate pulse generator (Princeton Instruments, Model PG-200). The gate pulse generator triggers the OMA and provides for delay of the gate pulse after the laser pulse and variation of the gate pulse width (integration time).

3 Results

Soil Compression Effects

A cone penetrometer inherently requires large forces to be applied to the soil in the immediate vicinity of the tip. To understand the effect of soil compression on LIBS measurements, soil samples contaminated with chromium were compressed, then allowed to relax for various periods before LIBS analysis. Sand samples (~75 g) were doped with 50 ppm Cr (w/w). Samples were then compressed in aluminum sample holders under a load of 177.92 kN (20 tons) for 1 min. Different samples were allowed to relax from 2 to 20 min before being analyzed using LIBS. Data for less than 2 min were not possible due to sample preparation location and the time required to perform the first LIBS measurements. Results of two trials are shown in Figure 5.

The emission intensity ratio of Cr-I (425.44 nm) to Si-I (390.55 nm) increases during the first 6 to 10 minutes before decreasing to a level approximately equal to the initial measurement. The notation Cr-I (425.44 nm) refers to the singly ionized chromium emission line at 425.44 nm wavelength. This notation is used throughout this report for other elements and their ionization emission.

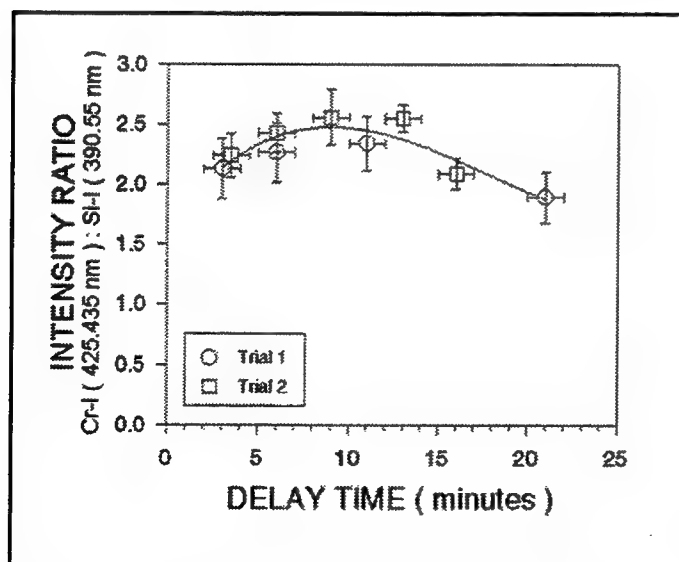


Figure 5. Effect of "relaxation time" after soil compression (177.92 kN (20 tons) for 1 min) on LIBS measurements of 50 ppm Cr in sand

Two competing processes are believed to be responsible for the observed time dependence of the measurements. One effect is related to the soil moisture content, which is known to decrease the intensity ratio as the moisture content increases. As the soil moisture increases, a greater portion of the laser pulse is required to excite water adsorbed on the sand granules.

As the soil is compressed, moisture is expelled from the soil matrix. During the relaxation period, humidity from the ambient air is readsorbed by the sand. A second contributing effect is due to energy being stored in the sand particles by the compression process. Since the energy introduced by the compression process is stored mainly in the silicon (silicon dioxide), there will be a trend for the silicon line intensity to increase over the chromium line intensity. In addition, any stored energy makes it easier to produce a slightly higher plasma temperature. The stored energy effect is not permanent and relaxes in time (~20 min).

Excitation Source

The relative importance of excitation laser wavelength used in the LIBS analysis was investigated by comparison of LIBS calibration data for Pb in a silt matrix. Samples with concentrations of Pb ranging from 100 to 2,000 ppm in silt were analyzed by LIBS with excimer ($\lambda = 248$ nm) and Nd:YAG ($\lambda = 1,064$ nm) lasers. The resulting calibration information is shown in Figure 6.

Lower detection limits were determined according to the relation $C_L = 2S/M$, where C_L is the lower detection limit, S is the sample standard deviation, and M is the slope of the calibration curve near the lower limit. Using this method, the values of C_L for the excimer and Nd:YAG lasers were 180 and 210 ppm, respectively. The slope of the calibration curve is greater for the excimer laser, suggesting a lower detection limit, but is offset by a greater standard deviation. This increased sample standard deviation is attributed to the relative instability of the excimer laser as compared with the Nd:YAG. Thus, no significant increase in detection limit can be expected by using an excimer laser instead of a Nd:YAG laser, even though the excimer-produced lines are generally better resolved. Additional results are presented in Figures 7-24.

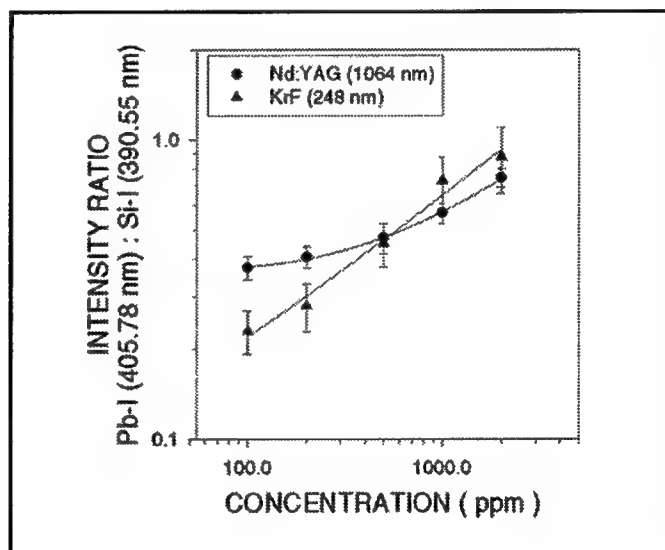


Figure 6. Comparison of calibration curves for Pb in clay, based on intensity ratio of Pb-I (405.78 nm) to Si-I (390.55 nm), obtained for Nd:YAG and excimer laser sources

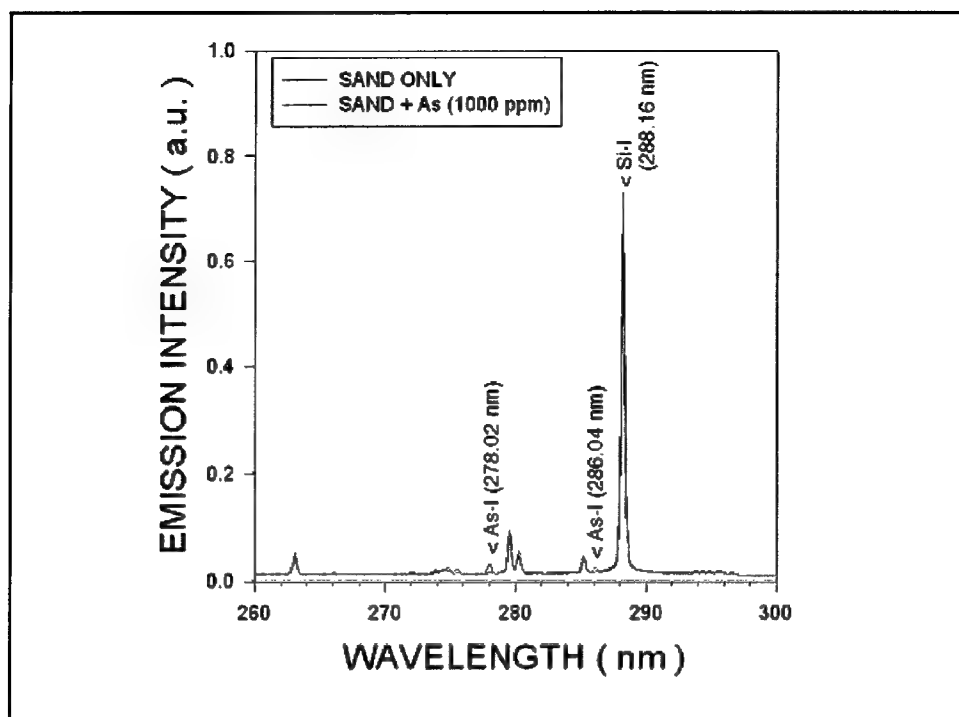


Figure 7. Emission spectrum showing relevant atomic emission lines of As and Si used in LIBS calibration

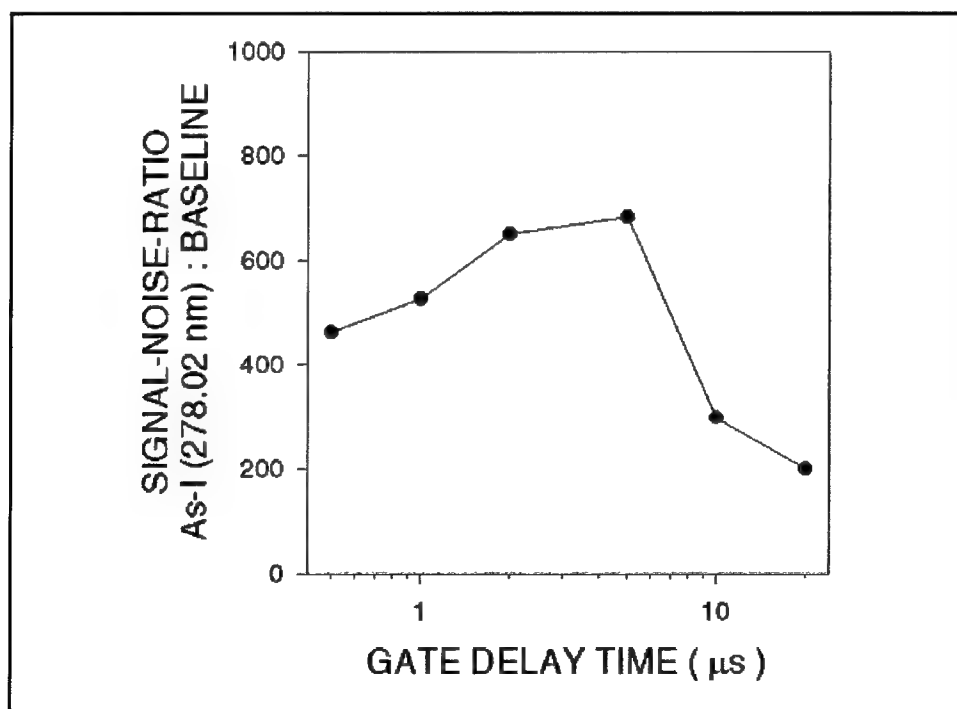
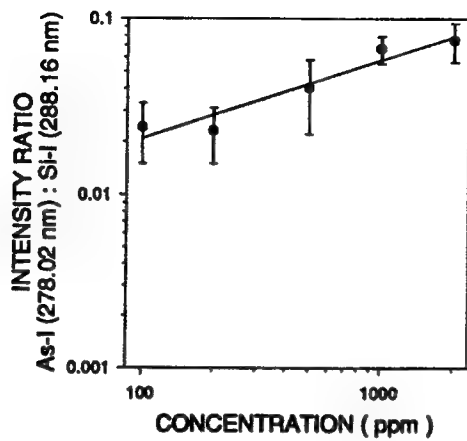
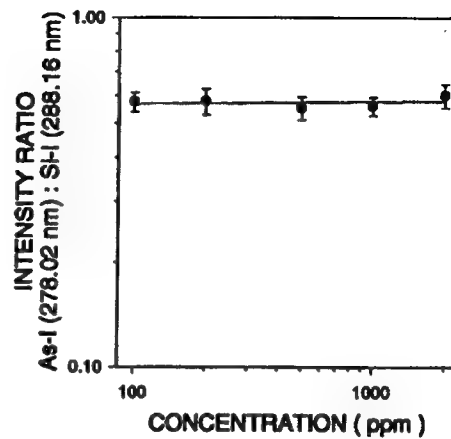


Figure 8. Plot of signal-noise ratio of As-I (278.02 nm) line to background in vicinity of 245 nm as a function of ICCD gate delay time

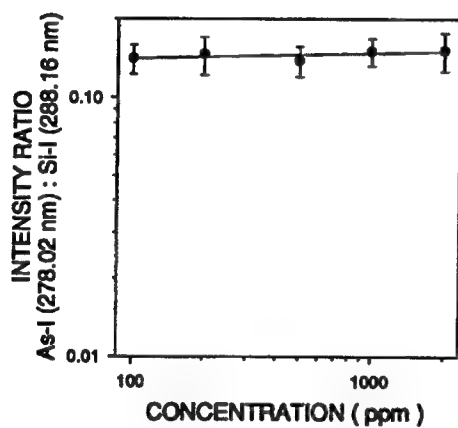
Arsenic (As)



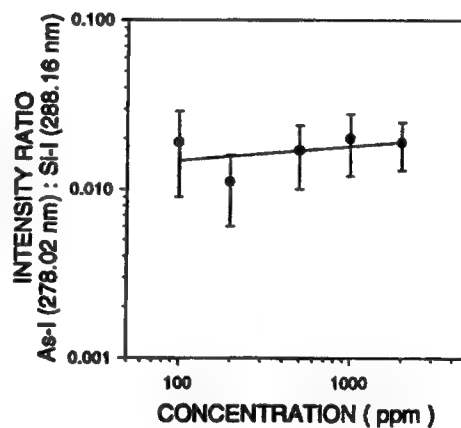
(a) Sand



(b) Silt



(c) Clay



(d) Kaolin

Figure 9. Calibration curves for As in (a) sand, (b) silt, (c) clay, and (d) kaolin, based on intensity ratio of As-I (278.02 nm) to Si-I (288.16 nm)

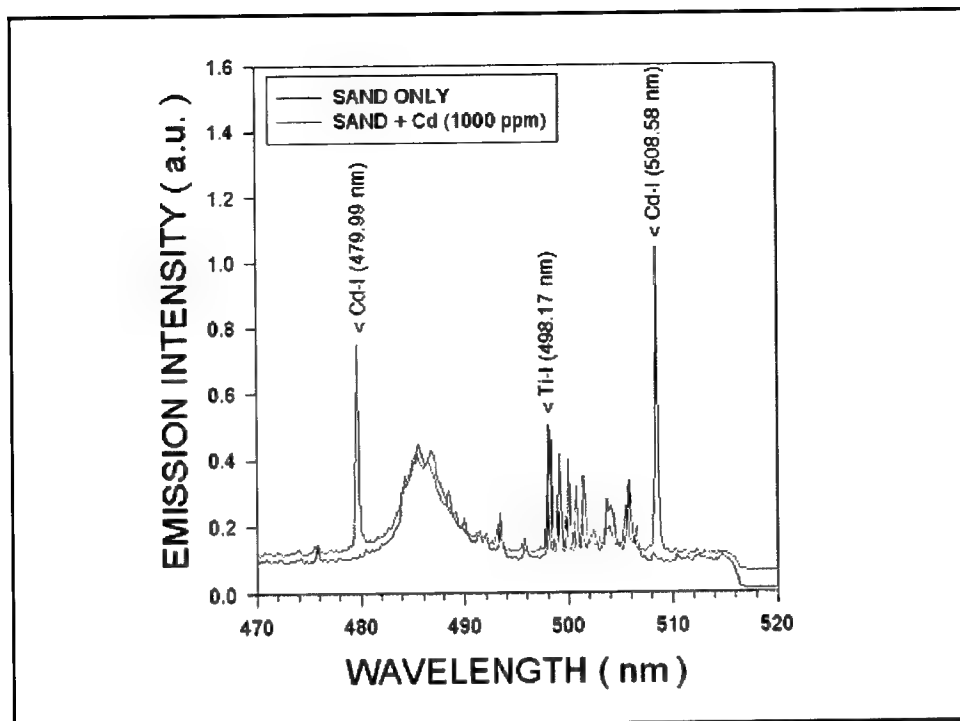


Figure 10. Emission spectrum showing relevant atomic emission lines of Cd and Ti used in LIBS calibration

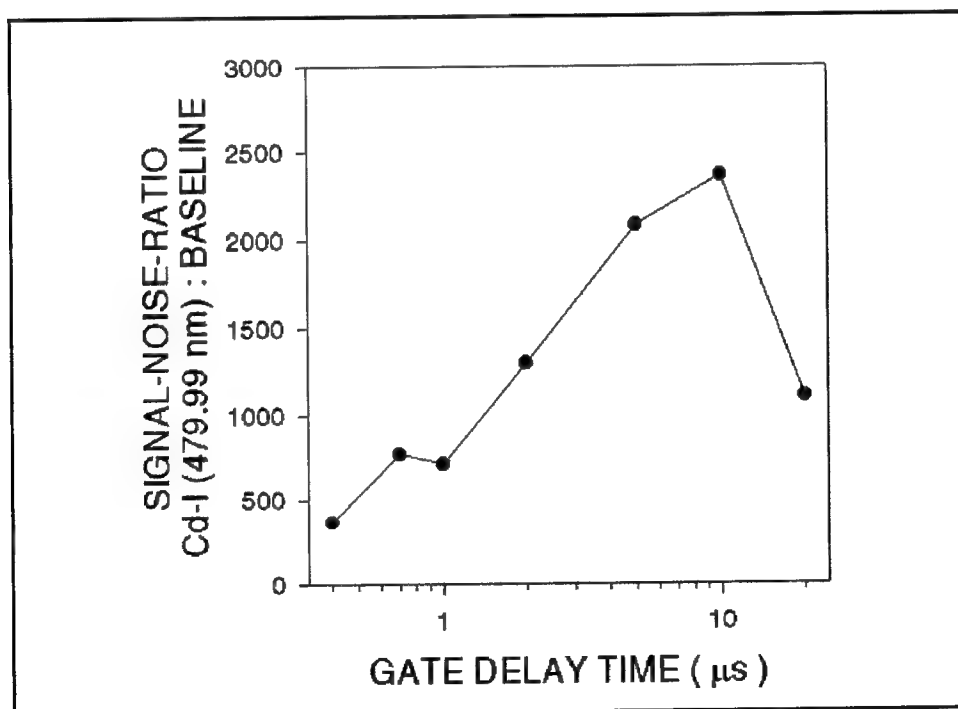
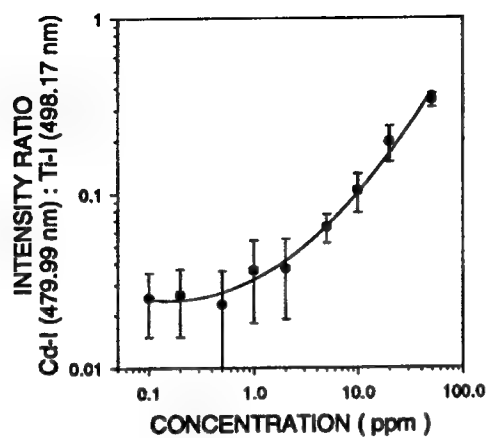
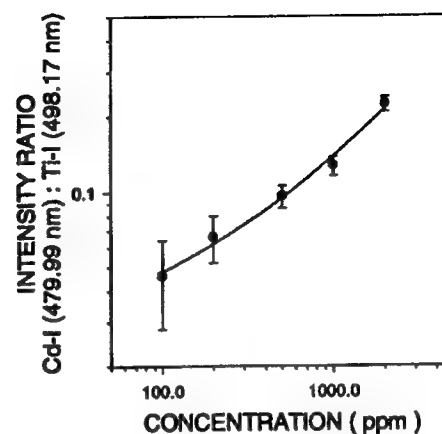


Figure 11. Plot of signal-noise ratio of Cd-I (479.99 nm) line to background in vicinity of 510 nm as a function of ICCD gate delay time

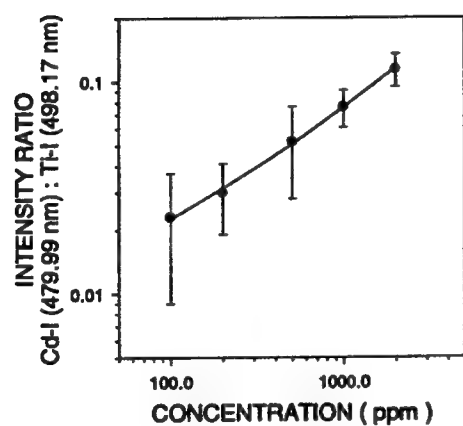
Cadmium (Cd)



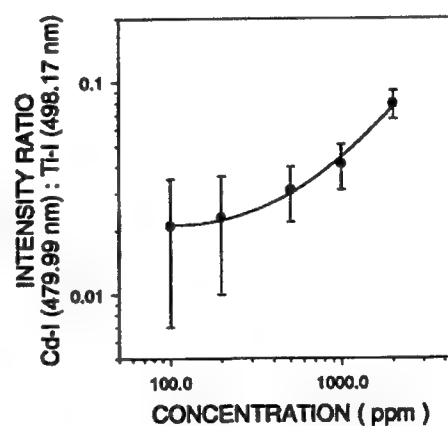
(a) Sand



(b) Silt



(c) Clay



(d) Kaolin

Figure 12. Calibration curves for Cd in (a) sand, (b) silt, (c) clay, and (d) kaolin, based on intensity ratio of Cd-I (479.99 nm) to Ti-I (498.17 nm)

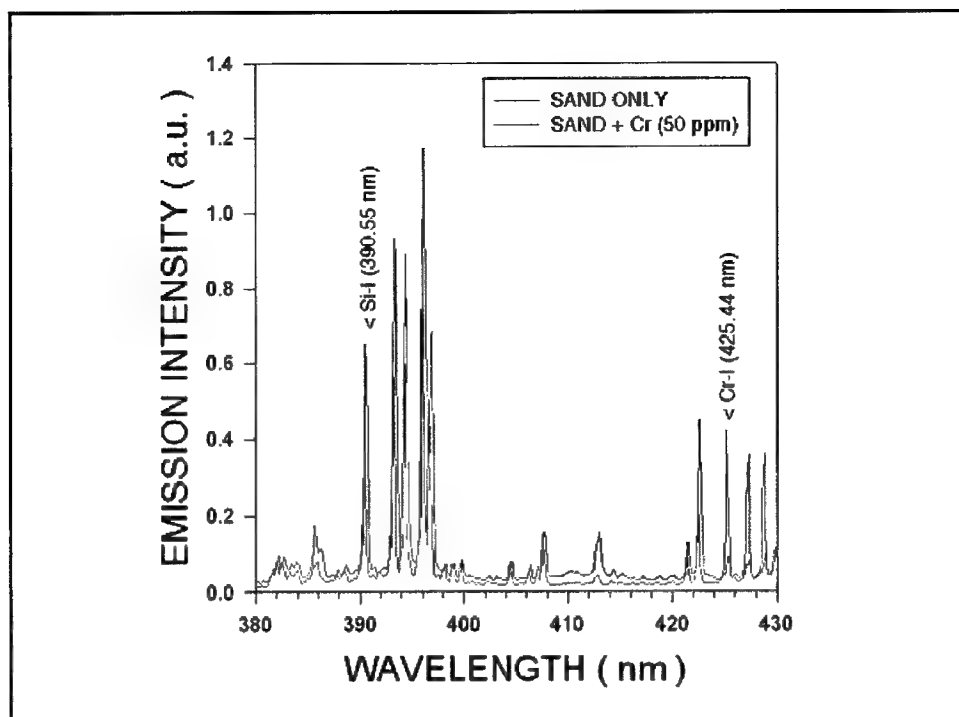


Figure 13. Emission spectrum showing relevant atomic emission lines of Cr and Si used in LIBS calibration

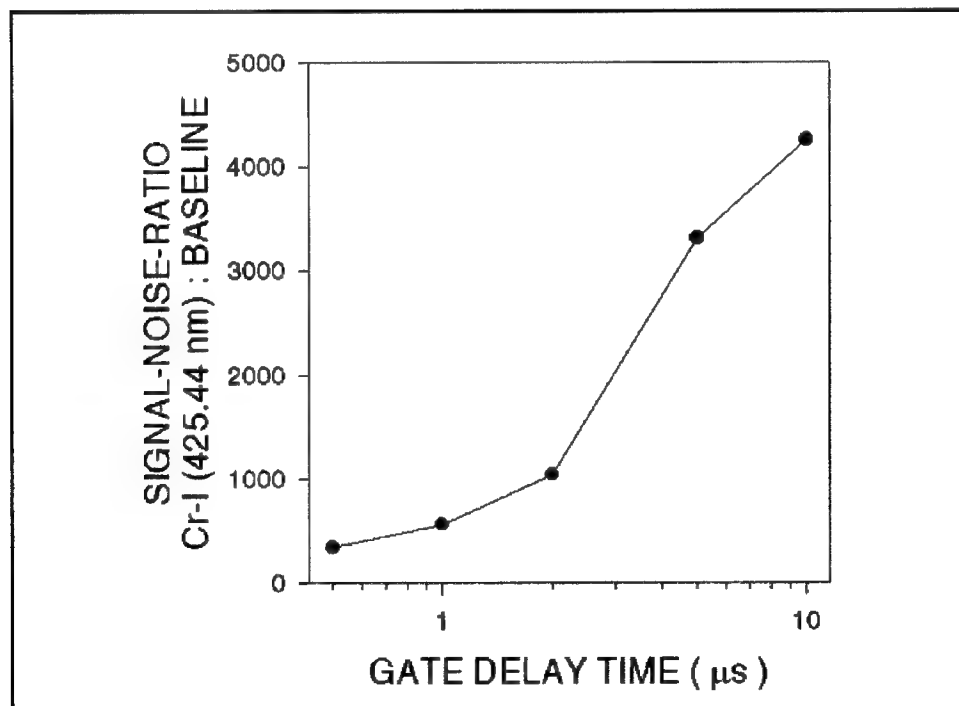
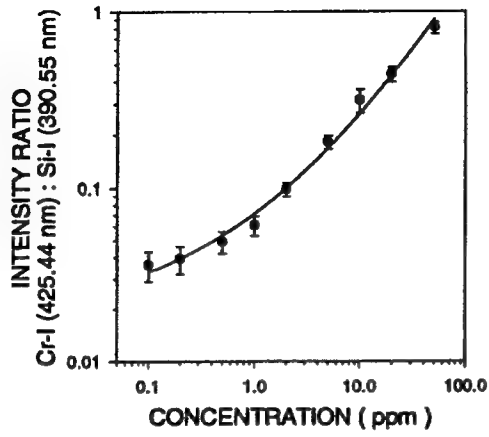
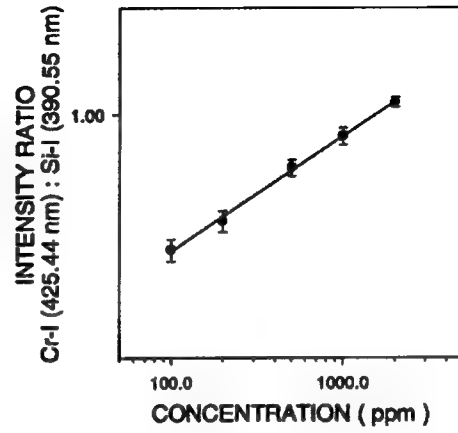


Figure 14. Plot of signal-noise ratio of Cr-I (425.44 nm) line to background in vicinity of 417 nm as a function of ICCD gate delay time

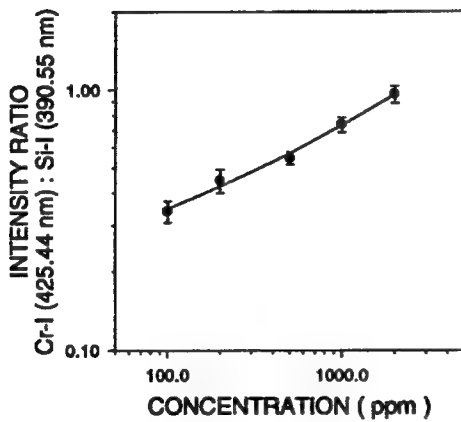
Chromium (Cr)



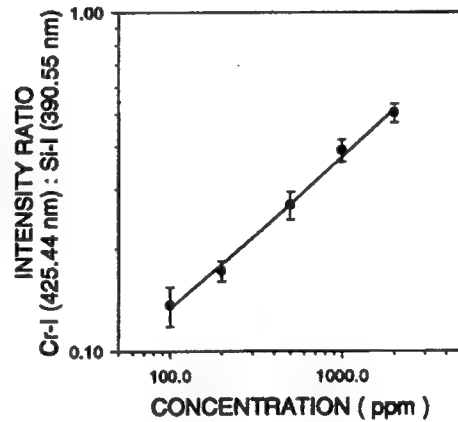
(a) Sand



(b) Silt



(c) Clay



(d) Kaolin

Figure 15. Calibration curves for Cr in (a) sand, (b) silt, (c) clay, and (d) kaolin, based on intensity ratio of Cr-I (425.44 nm) to Si-I (390.55 nm)

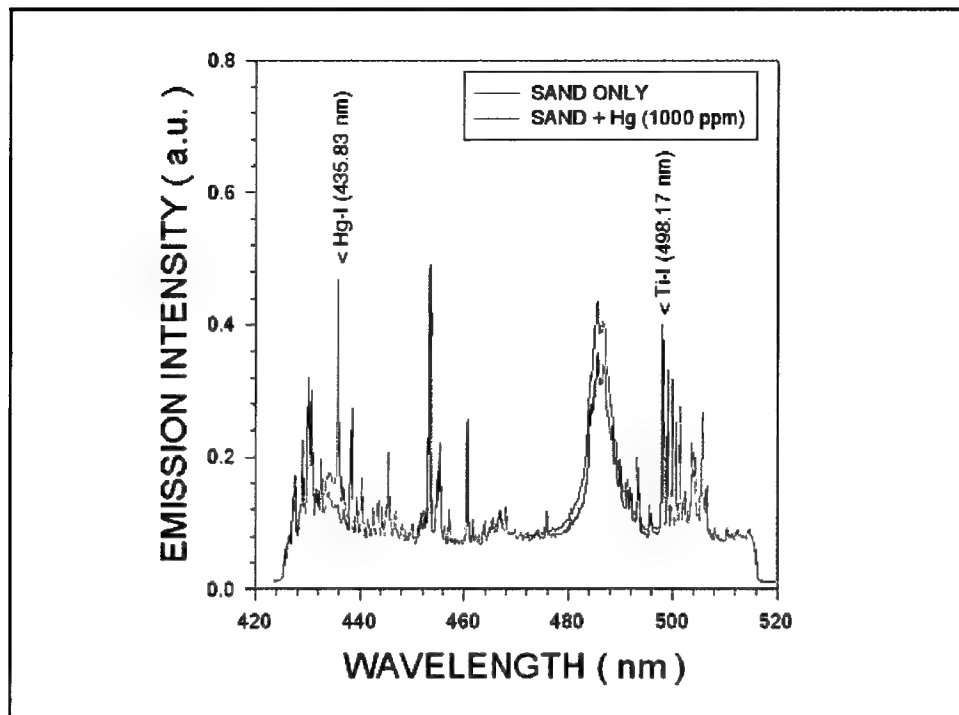


Figure 16. Emission spectrum showing relevant atomic emission lines of Hg and Ti used in LIBS calibration

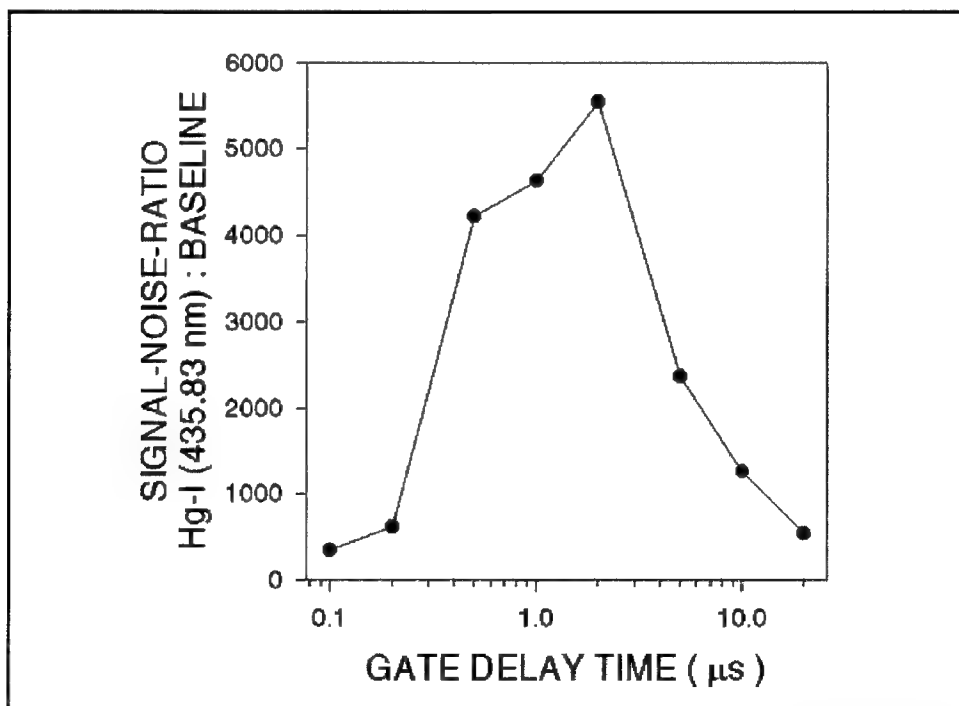
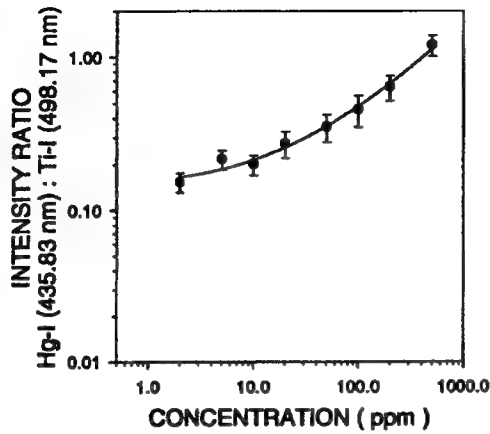
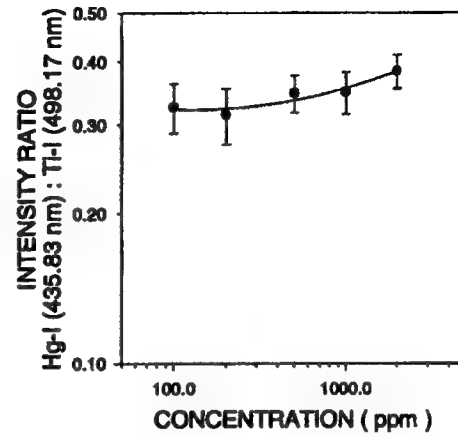


Figure 17. Plot of signal-noise ratio of Hg-I (435.83 nm) line to background in vicinity of 460 nm as a function of ICCD gate delay time

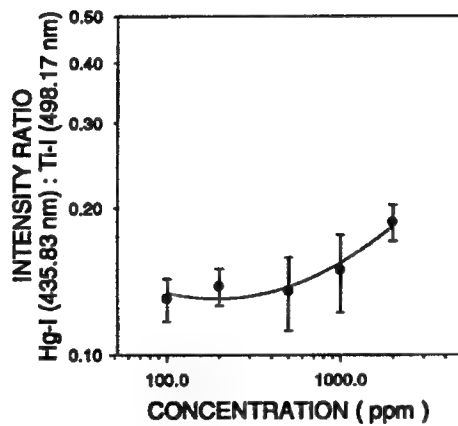
Mercury (Hg)



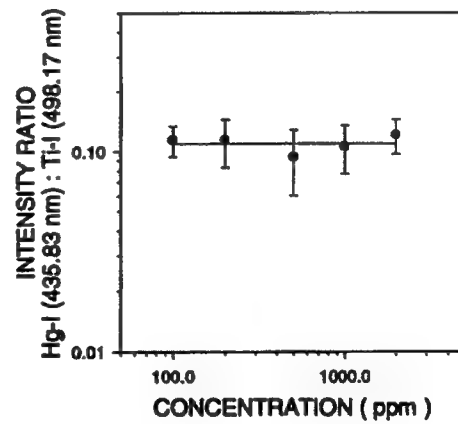
(a) Sand



(b) Silt



(c) Clay



(d) Kaolin

Figure 18. Calibration curves for Hg in (a) sand, (b) silt, (c) clay, and (d) kaolin, based on intensity ratio of Hg-I (435.83 nm) to Ti-I (498.17 nm)

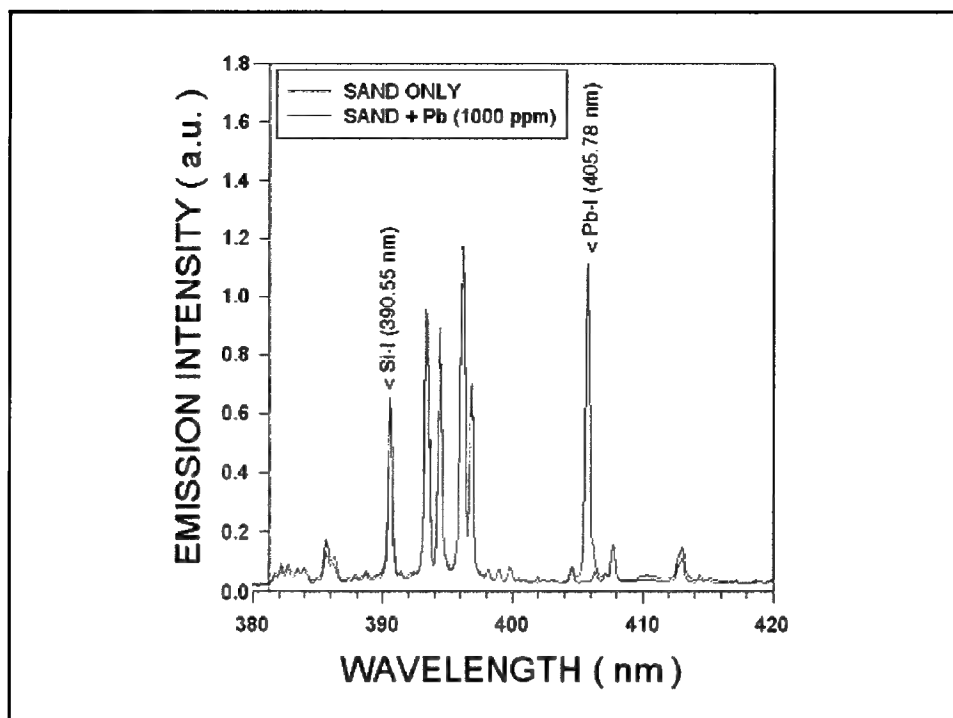


Figure 19. Emission spectrum showing relevant atomic emission lines of Pb and Si used in LIBS calibration

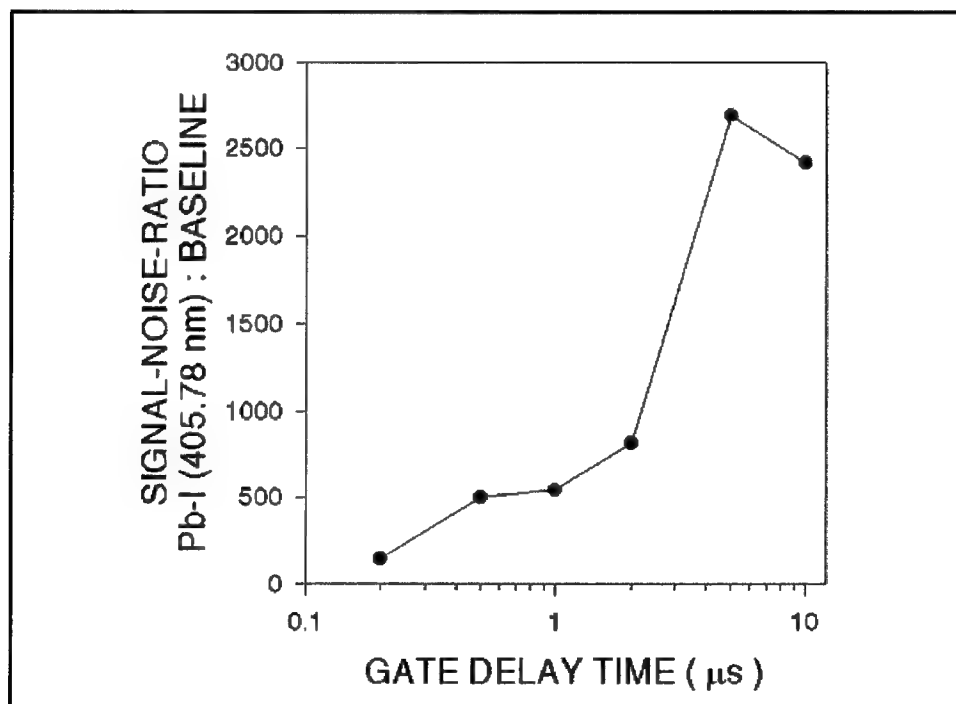
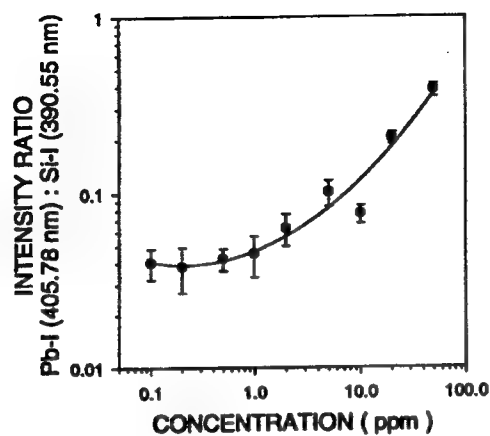
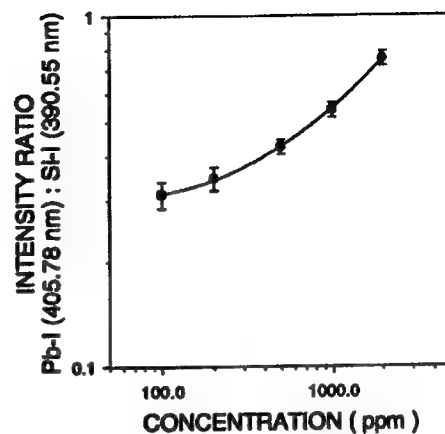


Figure 20. Plot of signal-noise ratio of Pb-I (405.78 nm) line to background in vicinity of 409 nm as a function of ICCD gate delay time

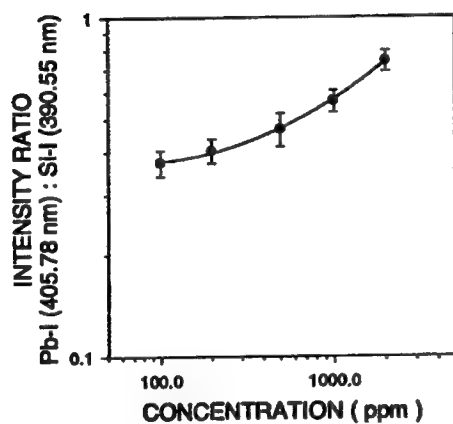
Lead (Pb)



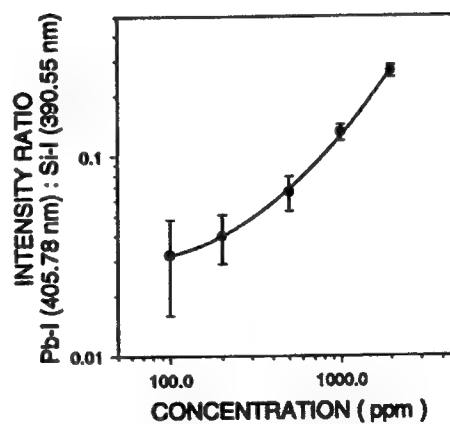
(a) Sand



(b) Silt



(c) Clay



(d) Kaolin

Figure 21. Calibration curves for Pb in (a) sand, (b) silt, (c) clay, and (d) kaolin, based on intensity ratio of Pb-I (405.78 nm) to Si-I (390.55 nm)

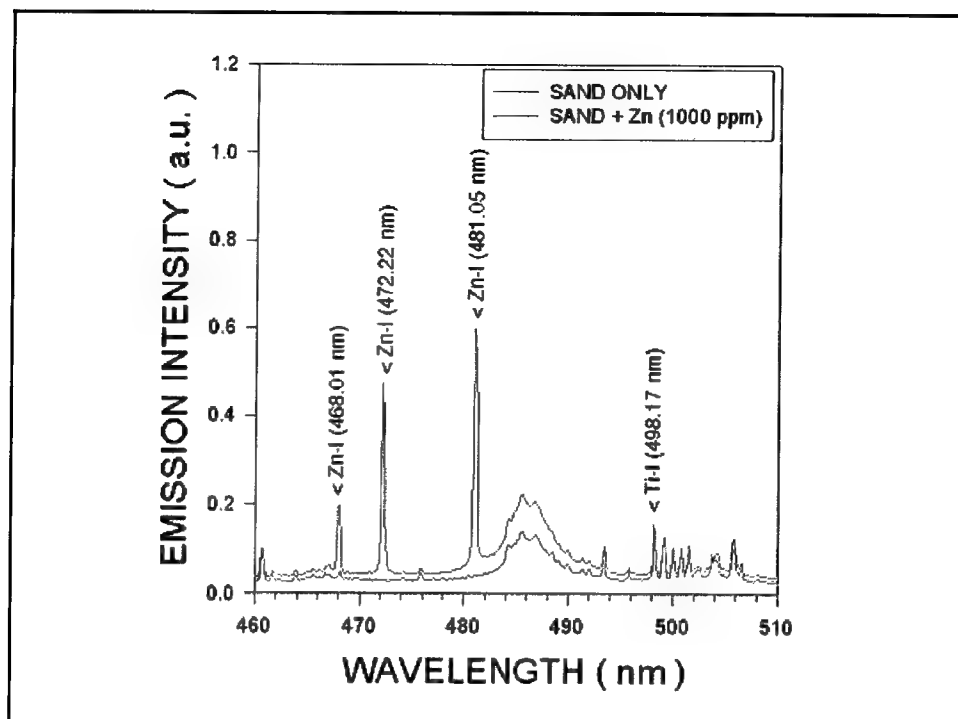


Figure 22. Emission spectrum showing relevant atomic emission lines of Zn and Ti used in LIBS calibration

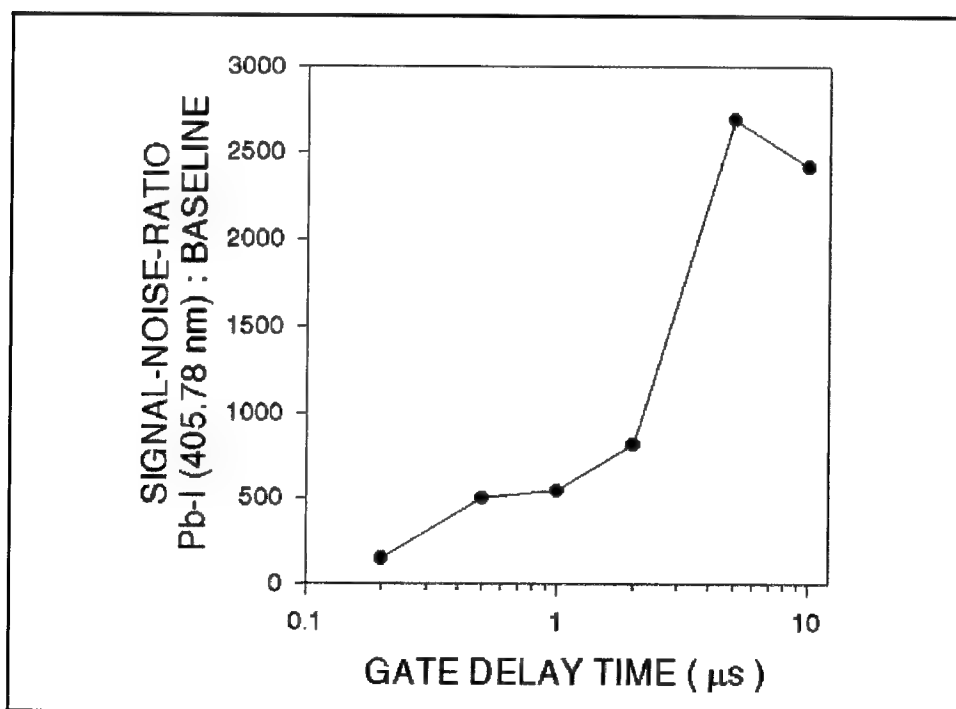
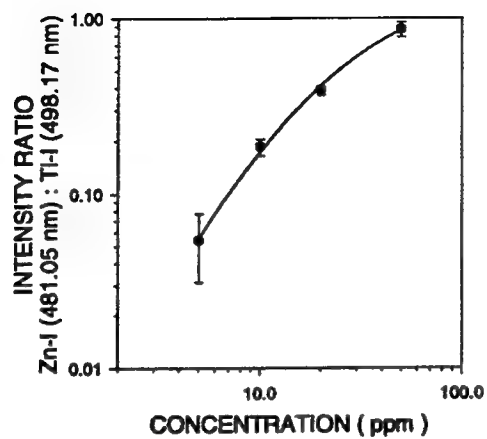
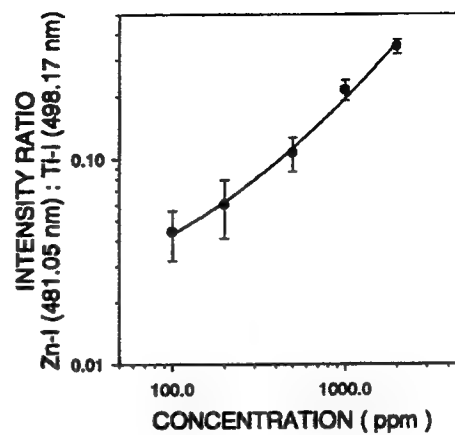


Figure 23. Plot of signal-noise ratio of Zn-I (481.05 nm) line to background in vicinity of 479 nm as a function of ICCD gate delay time

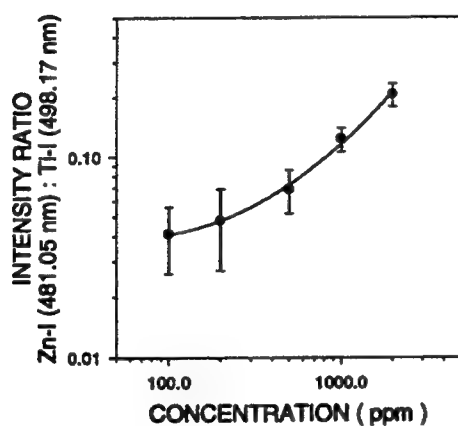
Zinc (Zn)



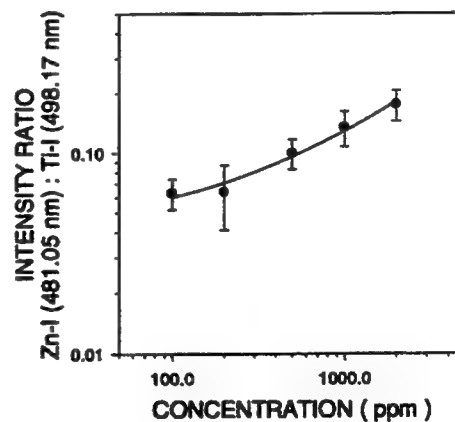
(a) Sand



(b) Silt



(c) Clay



(d) Kaolin

Figure 24. Calibration curves for Zn in (a) sand, (b) silt, (c) clay, and (d) kaolin, based on intensity ratio of Zn-I (481.05 nm) to Ti-I (498.17 nm)

Calibration Data

Calibration curves were developed for each of the heavy metals in sand, silt, clay, and kaolin with the following relevant instrument parameters.

Table 3
Relevant Instrument Parameters for LIBS Calibrations

Parameter	Value
Ambient temperature	22-24 °C
Ambient relative humidity	50-60 %
Laser pulse energy	125 mJ
Laser repetition rate	4 Hz
OMA slit width	10-20 µm
OMA grating (As, Cr, Pb)	600 g/mm, $\lambda_{\text{blaze}} = 300 \text{ nm}$
OMA grating (Cd, Hg, Zn)	600 g/mm, $\lambda_{\text{blaze}} = 450 \text{ nm}$
ICCD gate delay	2-5 µs
ICCD gate width	200 µs
ICCD gain	8.0
ICCD temperature	-40 °C

Detection Limits

Lower detection limits were derived from the calibration data according to the relation

$$C_L = \frac{2S}{M}$$

where

C_L = lower detection limit (concentration)

S = sample standard deviation

M = slope of calibration curve near lower limit

Results for each of the heavy metals, in each soil type, are shown in Table 4. Chromium was the most readily detectable element, followed by Pb, Zn, Cd, Hg, and with As being the least detectable. It is also evident that detection limits were 1 to 2 orders of magnitude lower in sand than in silt or clays. It has been suggested by Wisbrun et al. (1994) that this is due to the difference between surface contamination (as in sand) and volume contamination (as in silt and clays). Further investigations are needed to clearly resolve whether surface versus volume contamination is the cause

of these differences, or whether chemical reactions (resulting in different chemical bonds) may be affecting the LIBS measurements.

Table 4
Lower Detection Limits for As, Cd, Cr, Hg, Pb, and Zn in Sand, Silt, Clay, and Kaolin Samples

	Lower Detection Limit, ppm			
Element	Sand	Silt	Clay	Kaolin
As	530	†	†	†
Cd	3.3	160	360	830
Cr	0.42	74	73	83
Hg	11	1,800	1,100	†
Pb	1.4	150	210	340
Zn	1.6	190	510	300
Note: † = could not be determined from data.				

4 Conclusions

Calibration curves have been developed and lower detection limits determined for arsenic, cadmium, chromium, mercury, lead, and zinc in sand, silt, clay, and kaolin. All six elements were detectable in sand at concentrations approximately 2 orders of magnitude lower than in silt or clays. These results are in general agreement with work reported by WES and by Wisbrun et al. (1994).

Tests have been performed to demonstrate the variation of LIBS measurements as a function of soil compression and relaxation time. Results indicate that in the application of very accurate LIBS to cone penetrometer systems, one must take into account the time when the analysis is performed, since the LIBS results depend on the relaxation time between compression (cone penetrometer push) and LIBS analysis.

The importance of consistent methods for sample preparation ensuring more homogeneous samples in LIBS calibration work has been clearly demonstrated. It is unclear whether other LIBS results reported in the literature have followed such careful sample preparation.

No significant variations were found between LIBS measurements performed with an excimer laser and those performed with a Nd:YAG laser for the case of lead in silt.

References

- Alexander, D. R., Poulain, D. E., Kubik, R. D., and Ahmad, M. U. (1993). "Automated element identification in laser-induced breakdown spectroscopy studies of contaminated soils," Final Report to U.S. Army Engineer Waterways Experiment Station, Contract DACA39-93-K-0052.
- Alexander, D. R., Poulain, D. E., Khlif, M. S., and Cespedes, E. R. (1996). "Influences on detectability of heavy metals in soils by laser-induced breakdown spectroscopy," IGARSS'96, Lincoln, Nebraska (27-31 May 1996).
- Archontaki, H. A., and Crouch, S. R. (1988). "Evaluation of an isolated droplet sample introduction system for laser-induced breakdown spectroscopy," *Appl. Spectrosc.* 42, 741-746.
- Cremers, D. A., Barefield, J. E., II, and Koskelo, A. C. (1995). "Remote elemental analysis by laser-induced breakdown spectroscopy using a fiber-optic cable," *Appl. Spectrosc.* 49, 857-860.
- Cremers, D. A., and Radziemski, L. J. (1983). "Detection of chlorine and fluorine in air by laser-induced breakdown spectrometry," *Anal. Chem.* 55, 1252-1256.
- Cremers, D. A., Radziemski, L. J., and Loree, T. R. (1984). "Spectrochemical analysis of liquids using the laser spark," *Appl. Spectrosc.* 38, 721-729.
- Flower, W. L., et al. (1994). "A laser-based technique to continuously monitor metal aerosol emissions," *Fuel Proc. Tech.* 39, 277-284.
- Grant, K. J., Paul, G. L., and O'Neill, J. A. (1991). "Quantitative elemental analysis of iron ore by laser-induced breakdown spectroscopy," *Appl. Spectrosc.* 45, 701-705.
- Holtzclaw, K. W., Moore, J., and Senior, C. L. (1993). "Real-time optical measurement of alkali species in air for jet engine corrosion testing," *31st Aerospace Sciences Meeting & Exhibit*, Reno, NV.
- Ottesen, D. K., Baxter, L. L., Radziemski, L. J., and Burrows, J. F. (1991). "Laser spark emission spectroscopy for in situ, real-time monitoring of pulverized coal particle composition," *Energy & Fuels* 5, 304-312.

- Poulain, D. E., and Alexander, D. R. (1995). "Laser-induced breakdown spectroscopy of liquid aerosols: Droplet salt concentration measurements," *Appl. Spectrosc.* 49, 569-579.
- Radziemski, L. J., Loree, T. R., Cremers, D. A., and Hoffman, N. M. (1983). "Time-resolved laser-induced breakdown spectrometry of aerosols," *Anal. Chem.* 55, 1246-1252.
- Wachter, J. R., and Cremers, D. A. (1987). "Determination of uranium in solution using laser-induced breakdown spectroscopy," *Appl. Spectrosc.* 41, 1042-1048.
- Wisbrun, R., Schechter, I., Niessner, R., Schröder, H., and Kompa, K. L. (1994). "Detector for trace elemental analysis of solid environmental samples by laser plasma spectroscopy," *Anal. Chem.* 66, 2964-2975.

REPORT DOCUMENTATION PAGE

Form Approved
OMB No. 0704-0188

Public reporting burden for this collection of information is estimated to average 1 hour per response, including the time for reviewing instructions, searching existing data sources, gathering and maintaining the data needed, and completing and reviewing the collection of information. Send comments regarding this burden estimate or any other aspect of this collection of information, including suggestions for reducing this burden, to Washington Headquarters Services, Directorate for Information Operations and Reports, 1215 Jefferson Davis Highway, Suite 1204, Arlington, VA 22202-4302, and to the Office of Management and Budget, Paperwork Reduction Project (0704-0188), Washington, DC 20503.

1. AGENCY USE ONLY (Leave blank)	2. REPORT DATE June 1997	3. REPORT TYPE AND DATES COVERED Final report	
4. TITLE AND SUBTITLE Quantitative Analysis of the Detection Limits for Heavy Metal-Contaminated Soils by Laser-Induced Breakdown Spectroscopy		5. FUNDING NUMBERS 004DFN U433D40	
6. AUTHOR(S) Dennis R. Alexander, Dana E. Poulain			
7. PERFORMING ORGANIZATION NAME(S) AND ADDRESS(ES) University of Nebraska-Lincoln 248 WSEC, Box 880511 Lincoln, NE 68588-0511		8. PERFORMING ORGANIZATION REPORT NUMBER	
9. SPONSORING/MONITORING AGENCY NAME(S) AND ADDRESS(ES) U.S. Army Corps of Engineers Washington, DC 20314-1000; U.S. Army Engineer Waterways Experiment Station 3909 Halls Ferry Road, Vicksburg, MS 39180-6199		10. SPONSORING/MONITORING AGENCY REPORT NUMBER Miscellaneous Paper IRRP-97-2	
11. SUPPLEMENTARY NOTES Available from National Technical Information Service, 5285 Port Royal Road, Springfield, VA 22161.			
12a. DISTRIBUTION/AVAILABILITY STATEMENT Approved for public release; distribution is unlimited.		12b. DISTRIBUTION CODE	
13. ABSTRACT (Maximum 200 words) Laser-induced breakdown spectroscopy (LIBS) is a rapid remote measurement method for detection of metals in the environment. A major factor in the quantitative use of this technique involves the minimum detection limits under both laboratory and field operations. Research on limits of detection of heavy metals in different types of soils under various conditions using LIBS has been carried out under Contract DACA39-95-K-0053. Pulses from a Nd:YAG laser operating at 125 mJ at $\lambda = 1.06 \mu\text{m}$ are focused on sample surfaces to produce laser sparks (plasmas). Atomic emissions from the plasmas are recorded using an optical multichannel analyzer after delays of a few microseconds when interference from broadband emissions is reduced. Research has been performed on the detection limits of arsenic, cadmium, chromium, mercury, lead, and zinc in soil matrices. Results are reported on the lower detection limits of these six elements in sand, silt, clay, and kaolin matrices. Detection limits are significantly lower for heavy metals in sand matrices than silt and clay matrices due to differences between surface and volume contamination.			
14. SUBJECT TERMS Heavy metals Laser-induced breakdown spectroscopy		15. NUMBER OF PAGES 33 16. PRICE CODE	
17. SECURITY CLASSIFICATION OF REPORT UNCLASSIFIED	18. SECURITY CLASSIFICATION OF THIS PAGE UNCLASSIFIED	19. SECURITY CLASSIFICATION OF ABSTRACT	20. LIMITATION OF ABSTRACT